



**HAL**  
open science

## Direct conversion of CO<sub>2</sub> and CH<sub>4</sub> into liquid chemicals by plasma-catalysis

Di Li, Vandad Rohani, Frédéric Fabry, Aravind Parakkulam Ramaswamy,  
Mohamed Sennour, Laurent Fulcheri

► **To cite this version:**

Di Li, Vandad Rohani, Frédéric Fabry, Aravind Parakkulam Ramaswamy, Mohamed Sennour, et al..  
Direct conversion of CO<sub>2</sub> and CH<sub>4</sub> into liquid chemicals by plasma-catalysis. Applied Catalysis B:  
Environmental, 2020, 261, pp.118228. 10.1016/j.apcatb.2019.118228 . hal-02886661

**HAL Id: hal-02886661**

<https://minesparis-psl.hal.science/hal-02886661v1>

Submitted on 20 Jul 2022

**HAL** is a multi-disciplinary open access archive for the deposit and dissemination of scientific research documents, whether they are published or not. The documents may come from teaching and research institutions in France or abroad, or from public or private research centers.

L'archive ouverte pluridisciplinaire **HAL**, est destinée au dépôt et à la diffusion de documents scientifiques de niveau recherche, publiés ou non, émanant des établissements d'enseignement et de recherche français ou étrangers, des laboratoires publics ou privés.



Distributed under a Creative Commons Attribution - NonCommercial 4.0 International License

# Direct conversion of CO<sub>2</sub> and CH<sub>4</sub> into liquid chemicals by plasma-catalysis

Di Li<sup>1</sup>, Vandad Rohani<sup>1,\*</sup>, Frédéric Fabry<sup>1</sup>, Aravind Parakkulam Ramaswamy<sup>1</sup>, Mohamed Sennour<sup>2</sup>, Laurent Fulcheri<sup>1</sup>

*1. PSL Research University, MINES ParisTech, PERSEE - Centre Procédés, Énergies renouvelables et Systèmes énergétiques, 1 Rue Claude Daunesse, 06904 Sophia Antipolis, France*

*2. PSL Research University, MINES ParisTech, Centre des Matériaux, 63-65 rue Henri Auguste Desbrières - B.P. 87 à côté de SNECMA, 91003 Evry Cedex, France*

**Abstract:** A plasma-catalytic reactor consisting in a vertical coaxial dielectric barrier discharge reactor filled with solid catalysts was developed to directly synthesize liquid chemicals (alcohols, acids, hydrocarbons) and syngas from CO<sub>2</sub> and CH<sub>4</sub> at atmospheric conditions. Co and Fe catalysts prepared via incipient wetness impregnation method were loaded on a SiO<sub>2</sub> aerogel support synthesized by ambient drying method after surface modification. Discharges were generated in different ratios of CO<sub>2</sub>/CH<sub>4</sub> mixtures at ambient conditions and the performance of the catalysts was evaluated. In this study, the total liquid selectivity was approximately 40% after introducing the catalysts, where main liquid products were methanol and acetic acid. By varying the CH<sub>4</sub> and CO<sub>2</sub> ratio, a small number of long-chain hydrocarbons and alcohols were also detected with our catalysts. The synergy of plasma-catalysis in this process demonstrates great potential for the direct synthesis of value-added liquid chemicals and fuels from CO<sub>2</sub> and CH<sub>4</sub>.

**Keywords:** hydrocarbon synthesis, non-thermal plasma, liquid products, catalysts

## 1. Introduction

In recent centuries, the accumulation of greenhouse gases such as CO<sub>2</sub> and CH<sub>4</sub>, has contributed to climate change due to excessive emissions from fuel combustion, refinery plants, petrol industries, chemical industries, etc. Many techniques have been proposed to reduce the concentration of greenhouse gases as well as utilization, among those CO<sub>2</sub> capture has been regarded as an efficient one and is progressively applied in chemical and energy industries. However, storage of CO<sub>2</sub> still has significant issues regarding the high investment, transportation, and uncertainty of long-term storage [1]. Under this context, indirect and direct chemical conversion of CO<sub>2</sub> with CH<sub>4</sub> into value-added chemicals has attracted great attention and interest for its potential to achieve a sustainable and low carbon emission process in chemical and oil refinery industries and avoid the inconvenience of storage [2, 3]. For the indirect approach, which has been researched for decades, CO<sub>2</sub> and CH<sub>4</sub> mixture is first converted into syngas products. Then the syngas can be transformed into liquid fuels and other oxygenated chemicals by FTS process. For the more interesting direct approach, it is still a great challenge to us.

The thermodynamic stability of the CO<sub>2</sub> molecule is well known. The activation of CO<sub>2</sub> generally requires significant energy consumption, which makes the efficient activation and conversion of CO<sub>2</sub> a great challenge. Some researchers have focused their efforts on studying conventional thermochemical methods, including dry reforming to syngas, and direct conversion to liquid organics, associated with various catalysts. However, the essential high temperature and the deactivation of catalysts are critical issues and drawbacks [4]. In recent decades, non-thermal plasma (NTP) has been exploited and applied to various fields, such as degradation of pollutants and synthesis of chemicals, as it offers a unique pathway to induce thermodynamically unfavorable chemical reactions at a low temperature due to its high concentration of energetic and chemically active species [5]. The typical electron temperature (1-10 eV) of NTP is sufficient to activate CO<sub>2</sub> (5.5 eV) and CH<sub>4</sub> (4.5 eV) molecules into reactive radicals, excited molecules, atoms, and ions, which are energetic enough to initiate chemical reactions between CO<sub>2</sub> and CH<sub>4</sub>. Moreover, plasma discharge can be easily generated by applying voltage, where the renewables are holding more and more shares

in power generation. Therefore, the whole process can achieve a low emission and offer an alternative way to store renewable energy.

Enormous efforts have been dedicated to exploring the plasma-catalytic conversion of CO<sub>2</sub> with CH<sub>4</sub>, including studies on the effects of different plasma types, experimental variables and reactors to improve the conversion and selectivity to syngas products [6-17]. Moreover, various catalysts and packing materials have been investigated on plasma-catalytic reforming of CO<sub>2</sub> and CH<sub>4</sub>, including zeolites and some metal catalysts with their supports [18-23]. Tu et al. [24, 25] reported that full packing of Ni/Al<sub>2</sub>O<sub>3</sub> catalysts in the discharge volume could modify the discharge behavior from a typical filamentary discharge to a combination of surface discharges and spatially limited microdischarges, leading to a decrease of power in the discharge and conversion of reactants. Zou et al. [26] demonstrated the possibility that starch could directly enhance the oxygenate formation from methane and carbon dioxide. Scapinello et al. [27] explored the formation of carboxylic acids on the surface of copper and nickel electrodes. Other researchers also reported the formation of oxygenates as by-products in plasma-promoted reforming, although selectivity was still poor and external heating was essential [9, 28, 29]. Wang et al. [30] demonstrated the synthesis of a considerable production of liquid chemicals, including acetic acid, methanol, and acetone, via a novel DBD reactor equipped with a ground water electrode. They reported that the combination of a plasma process and Cu, Au, and Pt-Al<sub>2</sub>O<sub>3</sub> showed potential for the direct production of oxygenates under ambient conditions. However, most works mainly focused on the dry reforming of CO<sub>2</sub> and CH<sub>4</sub> into syngas production. Although the formation of methanol or formic acid has been reported by photocatalytic reduction of CO<sub>2</sub> [31-33], few efforts have been dedicated to plasma-catalytic synthesizing liquid chemicals (including hydrocarbons) directly from CO<sub>2</sub> and CH<sub>4</sub> with a considerable selectivity under ambient condition.

Formerly, our group has worked on the hydrocarbon synthesis through arc discharge at high pressures [34, 35]. In this study, we developed a plasma-catalytic reactor consisting of a vertical coaxial DBD reactor packing with metal doped SiO<sub>2</sub> aerogel catalysts, for the direct synthesis of liquid chemicals at ambient conditions. The metal catalysts we used in this work are Co and Fe, which are widely used in CO<sub>2</sub> hydrogenation and FTS process due to their high activity to CO<sub>2</sub> activation and chain propagation. The highly porous hydrophobic SiO<sub>2</sub> aerogel support was designed and

synthesized via ambient drying method after surface modification to avoid an extreme abatement in the discharge volume. The Co- and Fe-loaded SiO<sub>2</sub> aerogel catalysts were obtained by incipient wetness impregnation and then characterized. Finally, the catalysts were fully packed into the reactor, and the experimental study on catalytic performance was carried out and presented by comparing to no packing condition.

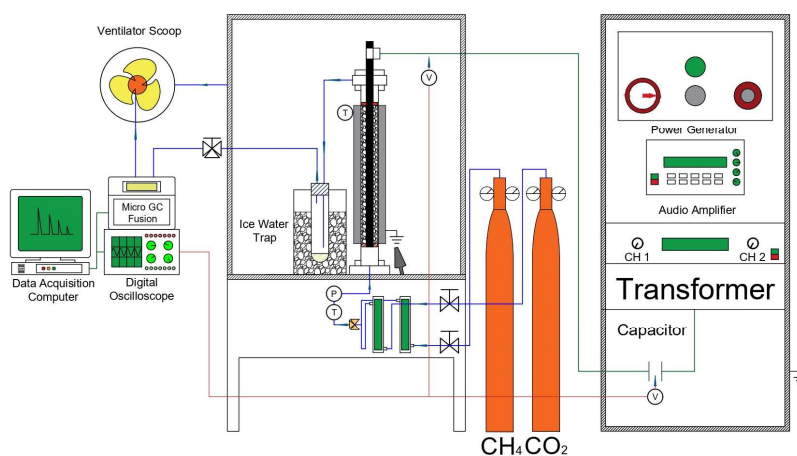
## **2. Methods and materials**

### *2.1. Experimental setup*

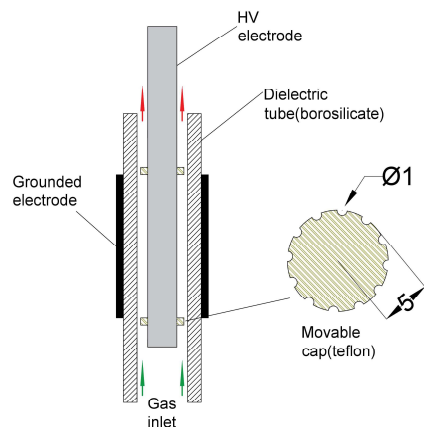
The schematic diagram of the setup is shown in Scheme 1. It was comprised of a power supply, a DBD reactor, a product collector, and an analysis system. The schematic diagram of the DBD reactor is presented in Scheme 2. The DBD reactor mainly included two coaxial electrodes and a dielectric ceramic tube. The inner high-voltage electrode was an aluminum rod with a diameter of 6 mm coaxially installed in the ceramic tube (10 mm i.d. × 12 mm o.d.); two evenly distributed adjustable Teflon caps (6 mm i.d. × 10 mm o.d.) with 12 semi-circle pores (1mm i.d.) were coupled with the aluminum rod to ensure the concentricity of the electrode in the ceramic tube and to fix the full-packed catalysts; the outer grounded electrode was a 200 mm-long stainless-steel coil wrapped around the dielectric tube. A compressed air gun was installed facing the reactor to avoid possible overheating; an IR camera (IRISYS IRI 4010) was used to measure and monitor the temperature of the reactor. The power supply system applied to the reactor was composed of a signal function generator (HP 33120A), an audio amplifier (IMG Stageline STA-1400) and a transformer. The amplifying output level range of the audio amplifier varies from “-80 dB” to “0 dB”, therefore the peak-to-peak voltage can be adjusted. Five different signals with a variable frequency can be generated through the function generator. In this work, the frequency of the sinusoidal signal was fixed at 3 kHz, and the peak-to-peak voltage was fixed at 5.5 kV. The Lissajous method was applied to calculate the applied power by connecting a capacitor (3.9 nF) in series with the reactor. Two high-voltage probes were applied to measure the voltage of the plasma reactor and the capacitor; two temperature probes were installed inside the reactor’s gas inlet and outlet respectively to measure the temperature of the inlet and outlet gas; one pressure probe was installed before the gas

inlet to monitor the pressure of inlet gas. The real-time temperature and pressure data were monitored and recorded simultaneously on a computer via a Keysight 34970A Data Acquisition unit. The electrical data were monitored in real time via a digital oscilloscope (HP Hewlett Packard 54615B) and recorded by the computer separately. The data files were recorded by 1,000 points for each of 2 channels once.

The gaseous products were analyzed online by a micro gas chromatography (Micro GC Fusion) equipped with two channels (an Rt-Molsieve 5 Å, R 0.25mm, L 10m column and an Rt-Q-Bond, R 0.25mm, L12m column) and two thermal conductivity detectors (TCD). An icy water trap was used to condense the liquid products before the micro GC. The liquid products were analyzed offline using a gas chromatography-mass spectrometer (GCMS-QP2010, Shimadzu) equipped with a SUPEL-Q PLOT (R 0.32mm, L 30 m) column. The difference in gas volume before and after the discharge was measured at the outlet by a soap-film flowmeter.



Scheme 1. Schematic diagram of the experimental setup.



Scheme 2. Schematic diagram of the DBD reactor.

## 2.2. Materials and analysis

The silica aerogel support was prepared using polyethoxydisiloxane (P75W20, PCAS, <30%) as silica precursors via a sol-gel method. 10 g of P75W20 was added to 15 g of ethanol (Fisher Scientific, Absolute) in a polyethylene vial while stirring. The solution was kept for 5 mins, after which 2625  $\mu\text{L}$  of distilled water was added to act as a hydrolysis agent, and 2955  $\mu\text{L}$  of (3-Aminopropyl) triethoxysilane (APTES, Thermo Fisher, 98%) solution (APTES: Ethanol = 1:50) was added to adjust the pH value for gelation. The final mixture solution was covered and allowed to gel and age at 60  $^{\circ}\text{C}$  for 48 h. Following the aging, 35 mL of Hexamethyldisilazane (HMDZ, Acros Organics, 98%) was added to the silica gels and left covered for 3 nights at ambient conditions to remove the hydroxyl groups. In the next step, the hydrophobic silica gels were washed in ethanol 5 times (over 2 days) to remove excessive HMDZ. The final gels were then transferred into an oven and dried for 2h at 140  $^{\circ}\text{C}$ .

The  $\text{Co}/\text{SiO}_2$  and  $\text{Fe}/\text{SiO}_2$  aerogel catalysts with the targeted mass ratio of Co or Fe loading (10% metal to silica) were prepared by the incipient wetness impregnation method. The targeted ethanolic solution of  $\text{Fe}(\text{NO}_3)_2 \cdot 9\text{H}_2\text{O}$  and  $\text{Co}(\text{NO}_3)_2 \cdot 6\text{H}_2\text{O}$  (Acros Organics,  $\geq 99\%$ ) was mixed with the same volume of silica aerogels prepared by the sol-gel method and maintained impregnated for one night. In the next step, the samples were dried for 2h at 140  $^{\circ}\text{C}$  and then calcined in air at 400  $^{\circ}\text{C}$  for 5h with a heating rate of 10  $^{\circ}\text{C}/\text{min}$  to obtain Fe or Co silica aerogels. Before the experiments, the catalysts samples were reduced in an  $\text{H}_2/\text{N}_2$  (5%/95%) flow at 600  $^{\circ}\text{C}$  for 10 h with a heating rate of 10  $^{\circ}\text{C}/\text{min}$ .

The micro GC was calibrated for each gaseous component using standard gas cylinders with a wide range of concentrations. Based on the measurements of the micro GC and the difference in temperature, pressure, and flow rate before and during each experiment, the conversion rate ( $x$ ) of H<sub>2</sub> and CO can be calculated as follows:

$$x_{CH_4} = \frac{\text{moles of } CH_4 \text{ consumed}}{\text{moles of } CH_4 \text{ inlet}} \times 100 \% \quad (1)$$

$$x_{CO_2} = \frac{\text{moles of } CO_2 \text{ consumed}}{\text{moles of } CO_2 \text{ inlet}} \times 100 \% \quad (2)$$

The selectivity and yield of gaseous products can be calculated as:

$$S_{H_2} = \frac{\text{moles of } H_2 \text{ produced}}{2 \times \text{moles of } CH_4 \text{ consumed}} \times 100 \% \quad (3)$$

$$S_{CO} = \frac{\text{moles of } CO \text{ produced}}{\text{moles of } CO_2 \text{ consumed} + \text{moles of } CH_4 \text{ consumed}} \times 100 \% \quad (4)$$

$$Y_{H_2} = \frac{\text{moles of } H_2 \text{ produced}}{2 \times \text{moles of } CH_4 \text{ input}} \times 100 \% \quad (5)$$

$$Y_{CO} = \frac{\text{moles of } CO \text{ produced}}{\text{moles of } CO_2 \text{ input} + \text{moles of } CH_4 \text{ input}} \times 100 \% \quad (6)$$

$$S_{C_xH_y} = \frac{x \times \text{moles of } C_xH_y \text{ produced}}{\text{moles of } CO_2 \text{ consumed} + \text{moles of } CH_4 \text{ consumed}} \times 100 \% \quad (7)$$

The selectivity of CH<sub>4</sub> to CO is defined as:

$$S_{CH_4/CO} = \frac{\text{moles of } CO \text{ produced} - \text{moles of } CO_2 \text{ consumed}}{\text{moles of } CH_4 \text{ consumed}} \times 100 \% \quad (8)$$

The ratio of unsaturated hydrocarbons/saturated hydrocarbons can be calculated as:

$$R = \frac{\text{moles of unsaturated } C_{2-5}}{\text{moles of saturated } C_{2-5}} \times 100 \% \quad (9)$$

The carbon balance based on the inlet and outlet gas can be calculated as:

$$CB = \frac{\text{moles of } C \text{ outlet}}{\text{moles of } C \text{ inlet}} \times 100 \% \quad (10)$$

The GCMS was calibrated using a standard liquid sample (20 vol% of methanol, ethanol, acetic acid, acetone, and water) to quantify the main products, and the results were normalized by abstracting water. As the selectivity to deposition was negligible as elaborated in supporting document, the selectivity towards liquid organics can then be calculated due to:



$$S_{liquid} = 100\% - S_{CO} - S_{C_xH_y} \quad (11)$$

$$S_{C_xH_yO_z} = x * \text{mole\% of } C_xH_yO_z * S_{liquid} \quad (12)$$

The specific input energy (SIE) is defined as the formula following:

$$SIE = \frac{\text{Power of discharge}(kW)}{\text{Flow rate}(\frac{L}{min})} * 60(\frac{s}{min}) \quad (13)$$

The energy efficiency (EE) of the reactor based on the gas conversion is defined as the reactants converted per unit of applied power:

$$E_{CO_2} = \frac{\text{moles of } CO_2 \text{ consumed}}{\text{power}} \quad (14)$$

$$E_{CH_4} = \frac{\text{moles of } CH_4 \text{ consumed}}{\text{power}} \quad (15)$$

### 3. Results and discussion

#### 3.1. Plasma experiments without catalysts

The plasma experiments without catalysts were conducted using a variable CO<sub>2</sub>/CH<sub>4</sub> ratio at a total flow rate of 30 mL/min and a variable total flow rate with a fixed CO<sub>2</sub>/CH<sub>4</sub> ratio of 2:1. The temperature of the reactor obtained from the IR camera in all of the tests was around 55°C-65°C (Figure S4 of the supporting materials), which is far lower than the essential temperature to initiate the reaction of CO<sub>2</sub> and CH<sub>4</sub> according to the thermodynamic equilibrium calculation (Figure S1, S2 and S3 of the supporting materials). Hence, we consider that conventional thermochemical reactions did not contribute to the conversion of CO<sub>2</sub> and CH<sub>4</sub> [25]. The selectivity of gaseous products, conversion rate, and corresponding SIE are illustrated in Figure 1. Table 1 shows the applied power, selectivity of CH<sub>4</sub> to CO, and energy efficiency. CO, H<sub>2</sub>, and C2-5 hydrocarbons, mostly alkanes, were synthesized as the major products. Methanol, acetic acid, some other oxygenates and a significant peak of water were also detected in the liquid composition; however, the total selectivity towards liquid organics was only around 0.1 or even less (the detailed composition of selectivity towards liquid products is not listed). It should be noted that the water was one part generated through the reactions; the other part was condensed from the air when opening the condensing bottle due to the temperature difference. In addition, a very small amount of carbon deposit was found on the surface of the reactor and electrode in some of the plasma

experiments without catalysts, while only negligible carbon deposit was found after placing the aerogel catalysts. The CO<sub>2</sub>/CH<sub>4</sub> ratio significantly affected the conversion rate of the reactants and the distribution of the products. The CO<sub>2</sub> and CH<sub>4</sub> conversion rates (from 19.2% and 37.8% to 29.6% and 43.2%) and the selectivity towards CO and H<sub>2</sub> (from 49% and 39.3% to 75.7% and 50.8%) increased with the CO<sub>2</sub>/CH<sub>4</sub> ratio with almost the same SIE, while the selectivity towards C2-C5 hydrocarbons dramatically decreased (from 41.5% to 22.2%). The reactive species of CO<sub>2</sub> and CH<sub>4</sub> plasma, including CO, CO<sub>2</sub><sup>+</sup>, O, OH, and CH<sub>3</sub>, have been reported by some researchers [25, 30]. The initial steps for the electron-impact dissociation of CH<sub>4</sub> and CO<sub>2</sub> in a non-thermal plasma could be described as:



Simulation work on plasma methane conversion has revealed that reaction (17) is responsible for 79% of CH<sub>4</sub> dissociation, while reactions (18) and (19) contribute 15% and 5% respectively [36]. This indicates that one part of the generated H finally formed H<sub>2</sub> due to the selectivity towards H<sub>2</sub> shown in Figure 1, while another part of H may combine with O, leading to the formation of H<sub>2</sub>O or OH species. The recombination reactions of CH<sub>x</sub> with the subsequent radicals resulted in the formation of higher hydrocarbons and oxygenates. Increasing the CH<sub>4</sub> ratio indeed increased the reactive CH<sub>3</sub> radicals. Therefore, the selectivity towards C2-C5 alkanes significantly increased. It is notable that the ratio of unsaturated hydrocarbons to saturated hydrocarbons is negligible as shown in Table 1, indicating that the recombination reaction of H with unsaturated species was dominant in NTPs. Except for reaction (16), the vibrationally excited CO<sub>2</sub>(v) can also be generated in NTPs, and O radicals and H radicals can efficiently attack CO<sub>2</sub>(v) molecules to produce CO [5]:



However, recent simulation work [37] has demonstrated that the population of vibrational levels could be limited in DBD plasma, and the dominant CO<sub>2</sub>-splitting

mechanisms were direct electron impact dissociation. Based on this understanding, instead of attacking CO<sub>2</sub>(v) molecules, the highly active O radicals could mainly combine with H to produce OH radicals and attack CH<sub>4</sub> molecules, along with producing OH and CH<sub>3</sub> radicals in the DBD reactor. Subsequently, the OH radicals could contribute to the formation of oxygenates (methanol, acetic acid, etc.) and water. Thus, O radicals could play a vital role in DBD plasma conversion of CO<sub>2</sub> with CH<sub>4</sub>, and this explains the increase in the conversion rate, energy efficiency of both reactants, yield of syngas products with the increase of CO<sub>2</sub> ratio, and the higher conversion rate of CH<sub>4</sub> compared to CO<sub>2</sub>. Another evidence was that no O<sub>2</sub> components were detected in the outlet gas, even with the highest CO<sub>2</sub> ratio, due to the limitation of reaction (20). We also noticed that the increase in CO<sub>2</sub> ratio increased the selectivity of CH<sub>4</sub> to CO. CH<sub>3</sub>OH and CH<sub>2</sub>O radicals are known to be easily decomposed when the translational temperature increases [5]. Therefore, the CH<sub>x</sub>O radicals, which were generated via the recombination of O or OH with CH<sub>x</sub> and contributed to the formation of oxygenates and chain growth, can also finally decompose into CO, H<sub>2</sub>, and H<sub>2</sub>O, resulting in the production of syngas instead of liquid organics. The increase in the CO<sub>2</sub> ratio certainly increased the CH<sub>x</sub>O radicals, leading to more decomposition into CO. Regarding the low selectivity towards liquid organics, the reaction route of decomposition could be dominant in the gas phase in DBD plasma:



Increasing total flow rate will certainly reduce the residence time of reactants in the discharge area of the reactor, resulting in reducing the chance of reactant molecule to collide with electrons that had enough energy to for dissociation, leading to the decrease of discharge power at a certain input signal and the decrease of conversions. Meanwhile, the selectivity of CH<sub>4</sub> to CO<sub>2</sub> also reduced. The reasons could be the decrease in residence time and the lower translational temperature, which leads to less decomposition of oxygenated radicals and high total selectivity of liquid organics.

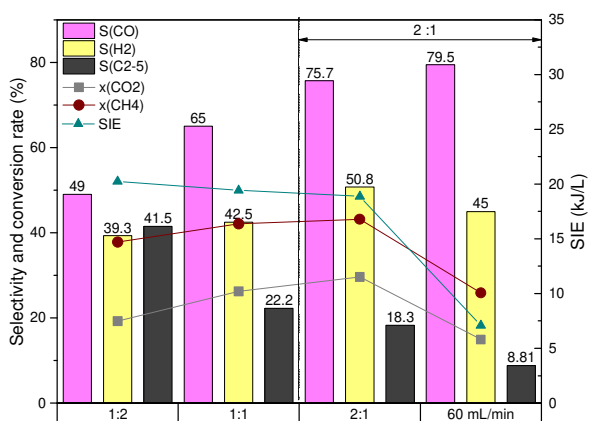


Figure 1. The selectivity of gaseous products, the conversion rates of reactants and the corresponding SIE varied by CO<sub>2</sub>/CH<sub>4</sub> ratio and total flow rate without catalysts (peak-to-peak voltage: 5.5 kV, frequency: 3 kHz).

Table 1. Applied power, the selectivity of CH<sub>4</sub> to CO, carbon balance, and the energy efficiency of the plasma experiments varied by CO<sub>2</sub>/CH<sub>4</sub> ratio and total flow rate without catalysts (peak-to-peak voltage: 5.5 kV, frequency: 3 kHz).

	S <sub>CH<sub>4</sub> to CO</sub>	R	Power (W)	EE (mmol/kJ)		Yield (%)		CB
				CO <sub>2</sub>	CH <sub>4</sub>	CO	H <sub>2</sub>	
1:2	0.357	0.051	10.1	0.129	0.508	15.44	14.85	0.983
1:1	0.414	0.037	9.71	0.276	0.442	22.00	17.87	0.966
2:1	0.513	0.033	9.45	0.427	0.311	26.57	21.91	0.984
60 mL/min	0.392	0.022	7.08	0.573	0.497	11.64	13.43	0.973

The plasma experiments with only CH<sub>4</sub> or CO<sub>2</sub> were also carried out without catalysts at the same peak-to-peak voltage, frequency, and total flow rate (30mL/min). As shown in Figure 2, the conversion rates of CH<sub>4</sub> only (28.6%) and CO<sub>2</sub> only (15.2%) experiments are much lower than those of the gas mixture. Considering that the recombination of O<sub>2</sub> and CO occurred in NTP conditions, it is reasonable that the conversion is lower than the tests of the gas mixture, in which the O mainly reacted with CH<sub>x</sub> and H radicals as mentioned above. As a result, the conversion of CH<sub>4</sub> seemed to be greatly promoted by O, while the conversion of CO<sub>2</sub> was relatively less promoted by H according to reaction (21), and the recombination of O<sub>2</sub> and CO was inhibited. The results confirmed that O was vital to the conversion of CH<sub>4</sub>. However, O<sub>2</sub>, as the main product of dissociation of CO<sub>2</sub>, was not found in the CO<sub>2</sub>/CH<sub>4</sub> plasma due to the activity of O<sub>2</sub> and the limitation of reaction (20). We also found that the carbon balance

of the CO<sub>2</sub>-only test was almost 100%, while with CH<sub>4</sub> only the carbon balance was around 95%. In fact, the threshold energy for the electron impact dissociation of CH<sub>4</sub> into carbon black (~14 eV) is much higher than the average electron energy of DBD, thus inhibiting the formation of carbon deposition. This indicated that CH<sub>4</sub> mainly attributed to the tiny amount of carbon black. Based on this analysis, the possible reaction pathway under these conditions is proposed as shown in Scheme 3.

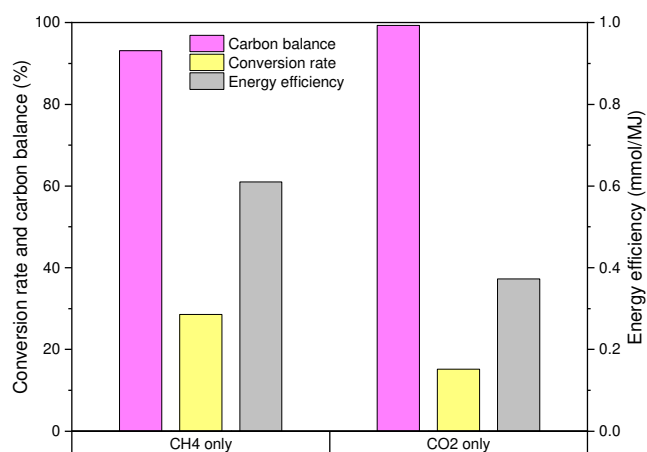
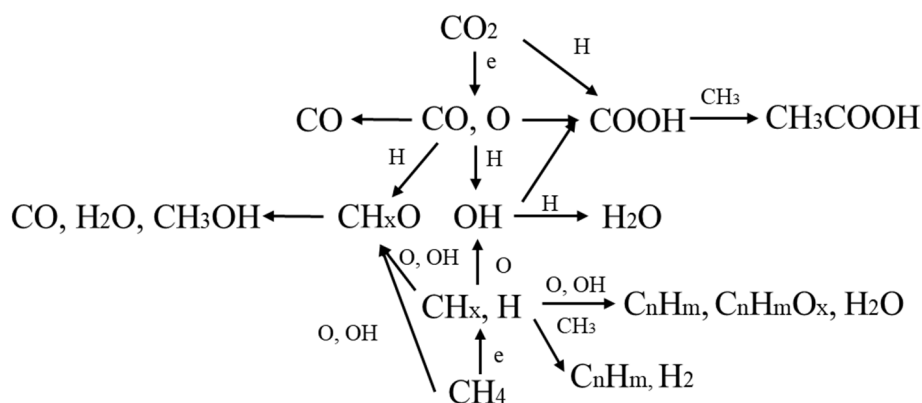


Figure 2. The carbon balance, conversion rates, and energy efficiency of CH<sub>4</sub>-only or CO<sub>2</sub>-only conditions without catalysts (peak-to-peak voltage: 5.5 kV, frequency: 3 kHz).



Scheme 3. Possible reaction pathways for the formation of gaseous and liquid products

### 3.2 Plasma experiments with catalysts

The plasma-catalytic experiments were carried out with reduced Co/SiO<sub>2</sub> aerogel and Fe/SiO<sub>2</sub> aerogel catalysts using a total flow rate of 30 mL/min, the same input electrical signal, and a variable CO<sub>2</sub>/CH<sub>4</sub> ratio. Figures 3 and 4 show the conversion rates, SIE, and energy efficiency without/with packing using a CO<sub>2</sub>/CH<sub>4</sub> ratio of 2:1

respectively; Figures 5 and 6 illustrate the corresponding selectivity of gaseous products and main liquid products respectively. As the selectivity towards liquid products is almost negligible compared to the experiments with packing, only the results with packing are listed. The total selectivity towards liquid without packing is shown in Table 1. Methanol, ethanol and acetic acid were detected as the main liquid products, while a small amount of acetone, 1-propanol, and methyl acetate was also found with the Co and Fe catalysts. Compared to no-packing conditions, introducing the SiO<sub>2</sub> aerogel support negligibly altered the conversion rates and the energy efficiency of CO<sub>2</sub> and CH<sub>4</sub>, while the selectivity towards methanol increased. Unlike Al<sub>2</sub>O<sub>3</sub> support [24], fully packing the SiO<sub>2</sub> aerogel support did not significantly alter the discharge behavior and decrease the conversions (Figure S5 of supporting materials). The reason could be the high sorption capacity of SiO<sub>2</sub> aerogel, which caused the sorption of reactive species, such as CH<sub>x</sub>O, into the mesoporous structure of silica aerogel (Table S1 of supporting materials), whereas previous simulation work [38] demonstrated that plasma was hardly formed. As a result, the decomposition of CH<sub>x</sub>O into CO could be inhibited, and the residence time could also increase, thus decreasing the selectivity of CH<sub>4</sub> to CO (from 0.513 to 0.369) and promoting the formation of liquid organics. We can also observe a difference between the SiO<sub>2</sub> aerogel support before and after the experiments (Figure S6 of the supporting materials). For further characterization of the deposition on the aerogels, which lead to the color change, TGA and XPS tests were conducted on the spent SiO<sub>2</sub> sample as shown in Figure S11, S12, and S13. It was found carbon-containing deposits including carbon deposition and carbon-containing polymers or monomers were formed on the surface of spent SiO<sub>2</sub> sample rather than only carbon black (Figure S12 and S13). Moreover, it was found that the overall selectivity towards carbon-containing deposits was less than 3% according to the TGA analysis (Figure S11). Therefore, it was not considered when calculating the selectivity to liquid products.

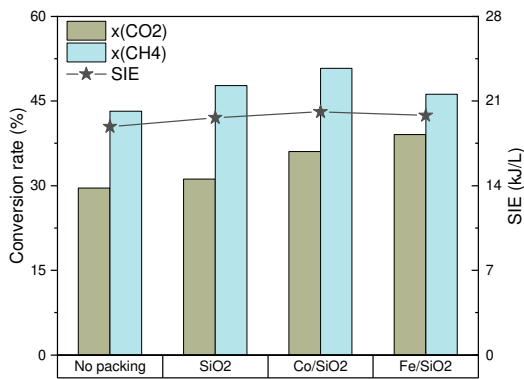


Figure 3. The conversion rates and SIE of the experiments without packing, with SiO<sub>2</sub> only, and with catalysts (peak-to-peak voltage: 5.5 kV, frequency: 3 kHz, total flow rate: 30 mL/min, CO<sub>2</sub>/CH<sub>4</sub> ratio = 2:1).

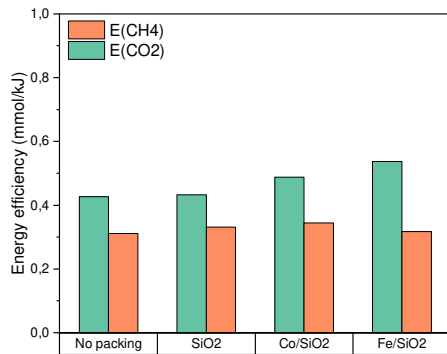


Figure 4. The energy efficiency of CO<sub>2</sub> and CH<sub>4</sub> without packing, with SiO<sub>2</sub> only, and with catalysts (peak-to-peak voltage: 5.5 kV, frequency: 3 kHz, total flow rate: 30 mL/min, CO<sub>2</sub>/CH<sub>4</sub> ratio = 2:1).

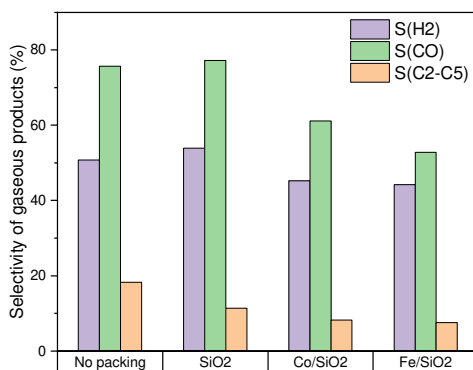


Figure 5. The selectivity of gaseous products without packing, with SiO<sub>2</sub> only, and with catalysts (peak-to-peak voltage: 5.5 kV, frequency: 3 kHz, total flow rate: 30 mL/min, CO<sub>2</sub>/CH<sub>4</sub> ratio = 2:1).

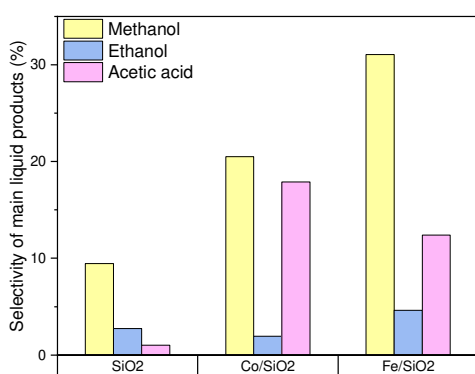


Figure 6. The selectivity of main liquid products without packing, with SiO<sub>2</sub> only, and with catalysts (peak-to-peak voltage: 5.5 kV, frequency: 3 kHz, total flow rate: 30 mL/min, CO<sub>2</sub>/CH<sub>4</sub> ratio = 2:1).

Introducing the Co or Fe catalyst with its SiO<sub>2</sub> aerogel support greatly promoted the formation of liquid organics compared to SiO<sub>2</sub> aerogel only or no packing, as shown in Figure 6. Moreover, the conversion rates and energy efficiency of CO<sub>2</sub> and CH<sub>4</sub> increased, while the selectivity towards gaseous products significantly decreased. We also noted that the Co and Fe catalyst exhibited effects on discharge behavior (Figure S4) due to an abatement of discharge volume and the modification of conductivity, resulting in a slight increase in discharge power. In addition to the mesoporous structure of the SiO<sub>2</sub> aerogel, the well-dispersed Co and Fe in the supports significantly affected the selectivity of the products and shifted them towards liquid organics (methanol up to 20.5% and 31.0%, acetic acid up to 17.9% and 12.4%). The synergistic effects between catalysts and plasma are quite complicated and debated. Possible explanations are: 1) the introduction of the catalysts altered the discharge behavior, leading to the transition to more stable surface discharge as shown in Figure S5 [39]; 2) the strong sorption behavior of the mesoporous structure in the support, as mentioned above, inhibited the decomposition of CH<sub>x</sub>O species; 3) the well-dispersed Co and Fe, two conventional catalysts used for the direct synthesis of long-chain products in conventional FTS and CO<sub>2</sub> hydrogenation process, remarkably enhanced the conversion of CO<sub>2</sub> and the formation of methanol and acetic acid. We also noted that Fe/SiO<sub>2</sub> was more favorable to alcoholic products with higher CO<sub>2</sub> conversion rates, while Co/SiO<sub>2</sub> favored the formation of acetic acid with a higher conversion rate of CH<sub>4</sub> when comparing the distribution of products between the two catalysts. Furthermore, more long-chain chemicals (propanol, methyl acetate) were detected in the liquid products via GC-MS



with packing Co/SiO<sub>2</sub> than packing Fe/SiO<sub>2</sub>. One possible explanation is that Co, as a widely used catalyst for chain growth in conventional FTS process, could be more capable of activating CH<sub>4</sub> into CH<sub>x</sub> and thus naturally more active in chain propagation. Meanwhile, Fe, which is well known to be capable of activating CO<sub>2</sub> in CO<sub>2</sub> hydrogenation process, could lead to more enrichment of OH radicals, which ultimately contribute to the formation of short-chain alcohols at low temperatures. For the characterization and comparison of deposition on Co/SiO<sub>2</sub> and Fe/SiO<sub>2</sub>, the C1s XPS spectra of catalyst samples and SiO<sub>2</sub> were normalized to compare the intensity as shown in Figure S14. The results indicated that the carbon-containing deposits were even much less formed on the Co/SiO<sub>2</sub> and Fe/SiO<sub>2</sub> samples than on the SiO<sub>2</sub> sample. Moreover, the peaking results of the corresponding C1s peaks (Figure S15) revealed that more organic deposition (polymer or monomer) rather than carbon deposition were formed on these catalyst samples.

Plasma-catalytic experiments with various CO<sub>2</sub>/CH<sub>4</sub> ratios were also conducted under the same conditions. The selective tendency of gaseous products that vary by CO<sub>2</sub>/CH<sub>4</sub> ratio with packing catalysts is similar to the results without packing catalysts as shown in Figure 8. Decreasing the CO<sub>2</sub>/CH<sub>4</sub> ratio logically leads to the generation of CH<sub>3</sub> radicals, therefore promoting the formation of long-chain products, such as ethanol, and decreasing the selectivity towards methanol. Indeed, more long-chain oxygenated species were detected, and hydrocarbons with particularly long chains (hexane, heptane) were found in the liquid products with the Co/SiO<sub>2</sub> catalyst (Figure S7 of supporting materials). Note that decreasing the CO<sub>2</sub>/CH<sub>4</sub> ratio significantly increased the selectivity towards acetic acid. As shown in Scheme 3, COOH radicals could be formed via the recombination of CO radicals with OH radicals and the combination of CO<sub>2</sub> and H radicals. Thus the selectivity towards acetic acid should logically decrease because fewer CO radicals and O radicals were generated in this condition. The results suggest that the catalysts could promote the conversion of CO<sub>2</sub> into COOH radicals instead of CH<sub>x</sub>O, and that production could depend more on H radicals than on CO<sub>2</sub>. It was clearly established once more that, whatever the ratio of CO<sub>2</sub>/CH<sub>4</sub>, the Co catalyst was more sensitive to acetic acid and long-chain products, while the Fe catalyst was more favorable to alcoholic products. Based on these results, we suggest that both Co and Fe are capable of activating the reactants and active to adsorb the radicals, especially O, OH, and CH<sub>x</sub> produced in NTP. Meanwhile, the

adsorbed  $\text{CH}_x$  can efficiently react with the adjacent OH to produce  $\text{CH}_x\text{O}$  and alcoholic products, mainly methanol. The adsorbed  $\text{CO}_2$  could react with the H radicals in the gas phase to produce COOH radicals, leading to the formation of organic acids, mainly acetic acid; the adsorbed  $\text{CH}_x$  and  $\text{CH}_x\text{O}$  would combine to form long-chain oxygenates (propanoic acid, butanol, etc.), or even react with H in the gas phase to produce long hydrocarbons and water, which in our study was responsible for the chain growth. Following this assumption, a possible pathway is proposed in Scheme 4. Significant results detected a small amount of hexane, heptane and C6 ester ( $\text{C}_6\text{H}_{12}\text{O}_2$ ) in liquid products using a  $\text{CO}_2/\text{CH}_4$  ratio of 2:1 with Co catalysts, while a small amount of pentanol and heptanol were found in the liquid products with Fe catalysts under the same conditions. Consequently, the direct synthesis of value-added liquid chemicals and syngas was achieved with interesting selectivity and energy efficiency via this plasma-catalytic process.

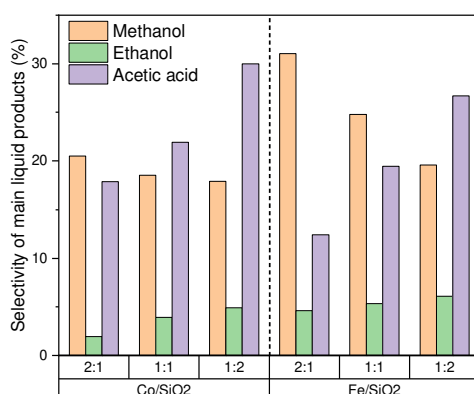


Figure 7. The selectivity of main liquid products as a function of catalysts and a  $\text{CO}_2/\text{CH}_4$  ratio from 2:1 to 1:2 (peak-to-peak voltage: 5.5 kV, frequency: 3 kHz, total flow rate: 30 mL/min).

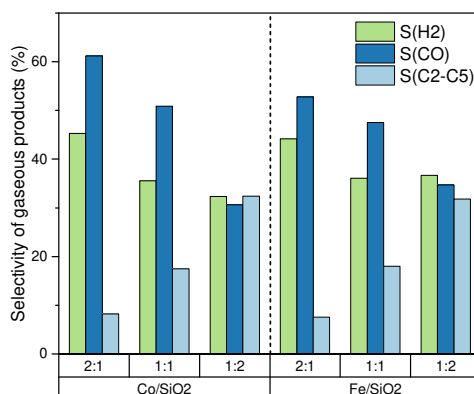
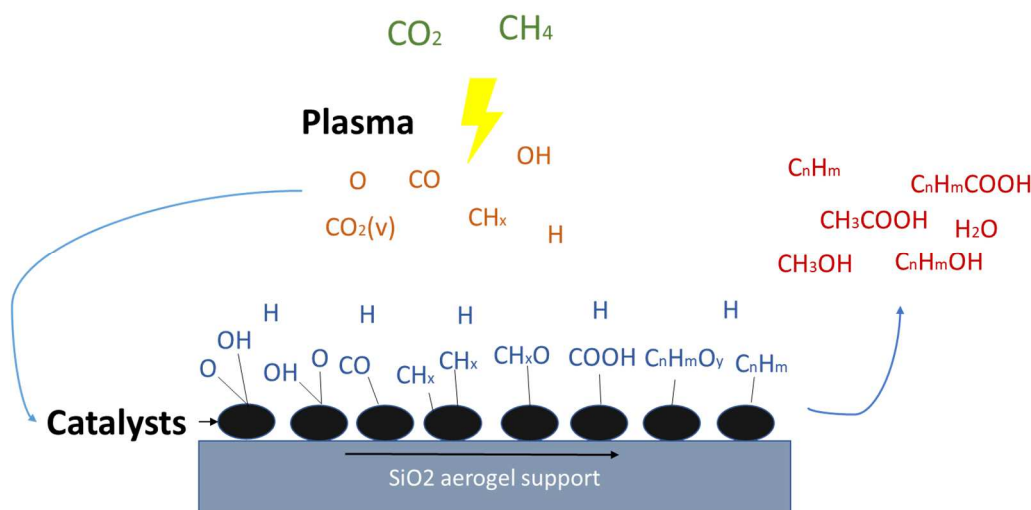


Figure 8. The selectivity of gaseous products as a function of catalysts and a CO<sub>2</sub>/CH<sub>4</sub> ratio from 2:1 to 1:2 (peak-to-peak voltage: 5.5 kV, frequency: 3 kHz, total flow rate: 30 mL/min).



Scheme 4. Possible reaction pathways for the formation of liquid products on the catalysts via plasma-catalytic approach.

## 4. Conclusion

In this study, the direct synthesis of value-added liquid chemicals from CO<sub>2</sub> and CH<sub>4</sub> by a plasma-catalytic process was achieved with considerable conversion rates at ambient conditions. The influence of different CO<sub>2</sub>/CH<sub>4</sub> ratios, SiO<sub>2</sub> aerogel packing, and supported catalysts packing was investigated.

Without packing, it was found that syngas and C<sub>2</sub> to C<sub>5</sub> gaseous hydrocarbons were the main products, while the total selectivity towards liquid products was negligible, mainly due to the decomposition of CH<sub>x</sub>O radicals. Increasing the CO<sub>2</sub>/CH<sub>4</sub> ratio increased the conversions of both reactants and the selectivity towards syngas, while selectivity towards C<sub>2</sub>+ species decreased.

With packing, the results were very different. Firstly, the use of aerogel as a support for the catalyst made it possible to avoid: (i) a significant abatement in discharge volume, (ii) an alteration of the discharge behavior. Moreover, due to its high sorption capacity, the packing version slightly favored the formation of liquid chemicals. Secondly, the synergetic addition of an appropriate catalyst in the system significantly promoted the formation of the liquid chemicals up to a total liquid selectivity of 40%, where methanol and acetic acid were the main liquid products. The results also revealed that the Fe catalyst preferentially led to the formation of alcoholic

products, while a Co catalyst was more favorable to the formation of acids and long-chain products (up to C5 oxygenates). Moreover, with a high ratio of CH<sub>4</sub>, a few C5+ hydrocarbons (pentane and heptane) and a C6 ester were synthesized. To our knowledge, the plasma-catalytic performance for liquid production obtained here is outstanding compared to existing studies and broadens the way to the design of an efficient plasma-catalytic process for direct conversion of CO<sub>2</sub> and CH<sub>4</sub> into liquid chemicals.

### **Conflict of interest**

The authors declare no competing financial interest.

### **Acknowledgments**

This research was carried out in the frame of the cooperative doctoral programs (ParisTech/CSC) supported by the China Scholarship Council (CSC). The authors warmly acknowledge CSC for their support.

### **Appendix A. Supporting materials**

## References

- [1] J. Koornneef, A. Ramírez, W. Turkenburg, A. Faaij, The environmental impact and risk assessment of CO<sub>2</sub> capture, transport and storage—An evaluation of the knowledge base, *Progress in Energy and Combustion Science*, 38 (2012) 62-86.
- [2] M. Aresta, A. Dibenedetto, A. Angelini, Catalysis for the valorization of exhaust carbon: from CO<sub>2</sub> to chemicals, materials, and fuels. Technological use of CO<sub>2</sub>, *Chemical reviews*, 114 (2013) 1709-1742.
- [3] C.W. Li, J. Ciston, M.W. Kanan, Electroreduction of carbon monoxide to liquid fuel on oxide-derived nanocrystalline copper, *Nature*, 508 (2014) 504.
- [4] Y.H. Hu, E. Ruckenstein, Catalytic conversion of methane to synthesis gas by partial oxidation and CO<sub>2</sub> reforming, *ChemInform*, 35 (2004) no-no.
- [5] A. Fridman, *Plasma chemistry*, Cambridge university press 2008.
- [6] Y. Yang, Methane conversion and reforming by nonthermal plasma on pins, *Industrial & engineering chemistry research*, 41 (2002) 5918-5926.
- [7] N. Seyed-Matin, A.H. Jalili, M.H. Jenab, S.M. Zekordi, A. Afzali, C. Rasouli, A. Zamaniyan, DC-pulsed plasma for dry reforming of methane to synthesis gas, *Plasma Chemistry and Plasma Processing*, 30 (2010) 333-347.
- [8] A. Aziznia, H.R. Bozorgzadeh, N. Seyed-Matin, M. Baghalha, A. Mohamadizadeh, Comparison of dry reforming of methane in low temperature hybrid plasma-catalytic corona with thermal catalytic reactor over Ni/ $\gamma$ -Al<sub>2</sub>O<sub>3</sub>, *Journal of Natural Gas Chemistry*, 21 (2012) 466-475.
- [9] J. Sentek, K. Krawczyk, M. Młotek, M. Kalczywska, T. Kroker, T. Kolb, A. Schenk, K.-H. Gericke, K. Schmidt-Szałowski, Plasma-catalytic methane conversion with carbon dioxide in dielectric barrier discharges, *Applied Catalysis B: Environmental*, 94 (2010) 19-26.
- [10] K.L. Pan, W.C. Chung, M.B. Chang, Dry reforming of CH<sub>4</sub> with CO<sub>2</sub> to generate syngas by combined plasma catalysis, *IEEE Transactions on Plasma Science*, 42 (2014) 3809-3818.
- [11] W.-C. Chung, K.-L. Pan, H.-M. Lee, M.-B. Chang, Dry reforming of methane with dielectric barrier discharge and ferroelectric packed-bed reactors, *Energy & Fuels*, 28 (2014) 7621-7631.
- [12] D. Li, X. Li, M. Bai, X. Tao, S. Shang, X. Dai, Y. Yin, CO<sub>2</sub> reforming of CH<sub>4</sub> by atmospheric pressure glow discharge plasma: a high conversion ability, *International Journal of Hydrogen Energy*, 34 (2009) 308-313.
- [13] H. Long, S. Shang, X. Tao, Y. Yin, X. Dai, CO<sub>2</sub> reforming of CH<sub>4</sub> by combination of cold plasma jet and Ni/ $\gamma$ -Al<sub>2</sub>O<sub>3</sub> catalyst, *international journal of hydrogen energy*, 33 (2008) 5510-5515.
- [14] L. Xiang, M.-g. BAI, X.-m. TAO, S.-y. SHANG, Y.-x. YIN, X.-y. DAI, Carbon dioxide reforming of methane to synthesis gas by an atmospheric pressure plasma jet, *Journal of Fuel Chemistry and Technology*, 38 (2010) 195-200.
- [15] A. Indarto, J.-W. Choi, H. Lee, H.K. Song, Effect of additive gases on methane conversion using gliding arc discharge, *Energy*, 31 (2006) 2986-2995.
- [16] Z. Bo, J. Yan, X. Li, Y. Chi, K. Cen, Plasma assisted dry methane reforming using gliding arc gas discharge: effect of feed gases proportion, *International Journal of Hydrogen Energy*, 33 (2008) 5545-5553.
- [17] X. Tu, J.C. Whitehead, Plasma dry reforming of methane in an atmospheric pressure AC gliding arc discharge: co-generation of syngas and carbon nanomaterials, *International Journal of Hydrogen Energy*, 39 (2014) 9658-9669.

- [18] K. Zhang, B. Eliasson, U. Kogelschatz, Direct conversion of greenhouse gases to synthesis gas and C4 hydrocarbons over zeolite HY promoted by a dielectric-barrier discharge, *Industrial & engineering chemistry research*, 41 (2002) 1462-1468.
- [19] K. Zhang, U. Kogelschatz, B. Eliasson, Conversion of greenhouse gases to synthesis gas and higher hydrocarbons, *Energy & fuels*, 15 (2001) 395-402.
- [20] T. Jiang, Y. Li, C.-j. Liu, G.-h. Xu, B. Eliasson, B. Xue, Plasma methane conversion using dielectric-barrier discharges with zeolite A, *Catalysis Today*, 72 (2002) 229-235.
- [21] K. Zhang, T. Mukhriza, X. Liu, P.P. Greco, E. Chiremba, A study on CO<sub>2</sub> and CH<sub>4</sub> conversion to synthesis gas and higher hydrocarbons by the combination of catalysts and dielectric-barrier discharges, *Applied Catalysis A: General*, 502 (2015) 138-149.
- [22] A.-J. Zhang, A.-M. Zhu, J. Guo, Y. Xu, C. Shi, Conversion of greenhouse gases into syngas via combined effects of discharge activation and catalysis, *Chemical Engineering Journal*, 156 (2010) 601-606.
- [23] F. Zhu, H. Zhang, X. Yan, J. Yan, M. Ni, X. Li, X. Tu, Plasma-catalytic reforming of CO<sub>2</sub>-rich biogas over Ni/ $\gamma$ -Al<sub>2</sub>O<sub>3</sub> catalysts in a rotating gliding arc reactor, *Fuel*, 199 (2017) 430-437.
- [24] X. Tu, H.J. Gallon, M.V. Twigg, P.A. Gorry, J.C. Whitehead, Dry reforming of methane over a Ni/Al<sub>2</sub>O<sub>3</sub> catalyst in a coaxial dielectric barrier discharge reactor, *Journal of Physics D: Applied Physics*, 44 (2011) 274007.
- [25] X. Tu, J. Whitehead, Plasma-catalytic dry reforming of methane in an atmospheric dielectric barrier discharge: Understanding the synergistic effect at low temperature, *Applied Catalysis B: Environmental*, 125 (2012) 439-448.
- [26] J.-J. Zou, Y.-p. Zhang, C.-J. Liu, Y. Li, B. Eliasson, Starch-enhanced synthesis of oxygenates from methane and carbon dioxide using dielectric-barrier discharges, *Plasma Chemistry and Plasma Processing*, 23 (2003) 69-82.
- [27] M. Scapinello, L.M. Martini, P. Tosi, CO<sub>2</sub> hydrogenation by CH<sub>4</sub> in a dielectric barrier discharge: catalytic effects of nickel and copper, *Plasma Processes and Polymers*, 11 (2014) 624-628.
- [28] V. Goujard, J.-M. Tatibouët, C. Batiot-Dupeyrat, Use of a non-thermal plasma for the production of synthesis gas from biogas, *Applied Catalysis A: General*, 353 (2009) 228-235.
- [29] K. Kozlov, P. Michel, H.-E. Wagner, Synthesis of organic compounds from mixtures of methane with carbon dioxide in dielectric-barrier discharges at atmospheric pressure, *Plasmas and Polymers*, 5 (2000) 129-150.
- [30] L. Wang, Y. Yi, C. Wu, H. Guo, X. Tu, One - step reforming of CO<sub>2</sub> and CH<sub>4</sub> into high - value liquid chemicals and fuels at room temperature by plasma - driven catalysis, *Angewandte Chemie International Edition*, 56 (2017) 13679-13683.
- [31] H. Takeda, H. Kamiyama, K. Okamoto, M. Irimajiri, T. Mizutani, K. Koike, A. Sekine, O. Ishitani, Highly Efficient and Robust Photocatalytic Systems for CO<sub>2</sub> Reduction Consisting of a Cu(I) Photosensitizer and Mn(I) Catalysts, *Journal of the American Chemical Society*, 140 (2018) 17241-17254.
- [32] X. Wang, X. Zhao, D. Zhang, G. Li, H. Li, Microwave irradiation induced UIO-66-NH<sub>2</sub> anchored on graphene with high activity for photocatalytic reduction of CO<sub>2</sub>, *Applied Catalysis B: Environmental*, 228 (2018) 47-53.
- [33] R. Yadav, V. Amoli, J. Singh, M.K. Tripathi, P. Bhanja, A. Bhaumik, A.K. Sinha, Plasmonic gold deposited on mesoporous Ti<sub>x</sub>Si<sub>1-x</sub>O<sub>2</sub> with isolated silica in lattice: An excellent photocatalyst for photocatalytic conversion of CO<sub>2</sub> into methanol under visible light irradiation, *Journal of CO<sub>2</sub> Utilization*, 27 (2018) 11-21.

- [34] S. Iwarere, V. Rohani, D. Ramjugernath, F. Fabry, L. Fulcheri, Hydrocarbons synthesis from syngas by very high pressure plasma, *Chemical Engineering Journal*, 241 (2014) 1-8.
- [35] V. Rohani, S. Iwarere, F. Fabry, D. Mourard, E. Izquierdo, D. Ramjugernath, L. Fulcheri, Experimental study of hydrocarbons synthesis from syngas by a tip–tip electrical discharge at very high pressure, *Plasma Chemistry and Plasma Processing*, 31 (2011) 663.
- [36] C. De Bie, B. Verheyde, T. Martens, J. van Dijk, S. Paulussen, A. Bogaerts, Fluid modeling of the conversion of methane into higher hydrocarbons in an atmospheric pressure dielectric barrier discharge, *Plasma Processes and Polymers*, 8 (2011) 1033-1058.
- [37] T. Kozák, A. Bogaerts, Splitting of CO<sub>2</sub> by vibrational excitation in non-equilibrium plasmas: a reaction kinetics model, *Plasma Sources Science and Technology*, 23 (2014) 045004.
- [38] Y.R. Zhang, K. Van Laer, E.C. Neyts, A. Bogaerts, Can plasma be formed in catalyst pores? A modeling investigation, *Appl. Catal. B-Environ.*, 185 (2016) 56-67.
- [39] D. Mei, X. Zhu, Y.-L. He, J.D. Yan, X. Tu, Plasma-assisted conversion of CO<sub>2</sub> in a dielectric barrier discharge reactor: understanding the effect of packing materials, *Plasma Sources Science and Technology*, 24 (2014) 015011.

Gas/Liquid product

CO<sub>2</sub>/CH<sub>4</sub>

